

October 2007

Stochastic optimization of low-loss optical negative-index metamaterial

Alexander V. Kildishev

Birck Nanotechnology Center, Purdue University, kildishev@purdue.edu

Uday K. Chettiar

Purdue University, uday@purdue.edu

Zhengdong Liu

Purdue University, liuzt@purdue.edu

V. M. Shalaev

Birck Nanotechnology Center and School of Electrical and Computer Engineering, Purdue University, shalaev@purdue.edu

Do-Hoon Kwon

Department of Electrical Engineering, Pennsylvania State University

See next page for additional authors

Follow this and additional works at: <http://docs.lib.purdue.edu/nanopub>

Kildishev, Alexander V.; Chettiar, Uday K.; Liu, Zhengdong; Shalaev, V. M.; Kwon, Do-Hoon; Bayraktar, Zikri; and Werner, Douglas H., "Stochastic optimization of low-loss optical negative-index metamaterial" (2007). *Birck and NCN Publications*. Paper 254.
<http://docs.lib.purdue.edu/nanopub/254>

This document has been made available through Purdue e-Pubs, a service of the Purdue University Libraries. Please contact epubs@purdue.edu for additional information.

Authors

Alexander V. Kildishev, Uday K. Chettiar, Zhengtong Liu, V. M. Shalaev, Do-Hoon Kwon, Zikri Bayraktar, and Douglas H. Werner

Stochastic optimization of low-loss optical negative-index metamaterial

Alexander V. Kildishev,^{1,*} Uday K. Chettiar,¹ Zhengtong Liu,¹ Vladimir M. Shalaev,¹ Do-Hoon Kwon,² Zikri Bayraktar,² and Douglas H. Werner²

¹Birck Nanotechnology Center, Purdue University, West Lafayette, Indiana 47907, USA

²Department of Electrical Engineering, Pennsylvania State University, University Park, Pennsylvania 16802, USA

*Corresponding author: kildishev@purdue.edu

Received March 6, 2007; accepted April 20, 2007;
posted April 24, 2007 (Doc. ID 80573); published July 20, 2007

Optical metamaterial consisting of metal-dielectric composites creates a complicated system that is not amenable to analytical solutions. This presents a challenge in optimizing these intricate systems. We present the application of three nature-inspired stochastic optimization techniques in conjunction with fast numerical electromagnetic solvers to yield a metamaterial that satisfies a required design criterion. In particular, three stochastic optimization tools (genetic algorithm, particle swarm optimization, and simulated annealing) are used for designing a low-loss optical negative index metamaterial. A negative refractive index around $-0.8+0.2i$ is obtained at a wavelength of 770 nm. The particle swarm optimization algorithm is found to be the most efficient in this case. © 2007 Optical Society of America

OCIS codes: 160.4670, 260.5740.

1. INTRODUCTION

This paper deals with the approaches to the computer-aided optimal design of novel metamaterials for parallel nanoscale optical sensing and imaging. The proposed approaches go together with the rapidly evolving techniques for fabricating optical metamaterials with novel exotic properties never before seen in nature. One of the most promising optical metamaterials for imaging applications to date is the negative index metamaterial (NIM). To make the subwavelength resolution possible, the refractive index of a given NIM ($n = \sqrt{\epsilon\mu}$) should satisfy the condition $n = -n_h$, where n_h is the refractive index of the host medium [1]. For operating on a scale much less than the wavelength of light, a simplification is possible, because for a small object electric and magnetic fields are decoupled so that only $\epsilon = -\epsilon_h$ is needed. Here such a lens is referred to as a near-field lens (NFL). The NFL operational frequency defined by the condition $\epsilon(\omega, p) = -\epsilon_h$ depends on the metal filling factor p and thus can be controlled by varying p . This makes it possible to tune the NFL to any wavelength across the visible and infrared parts of the spectrum [2]. This is in striking contrast to the NFL based on a layer of bulk metal, where the condition $\epsilon = -\epsilon_h$ can be fulfilled only for one fixed frequency (for the best NFL material, silver, the condition $\epsilon = -1$ occurs in the ultraviolet, at $\lambda \approx 340$ nm) [3,4]. Ultimate design of NFLs is one of several important applications for our optimization techniques.

Most of the designs suggested for NIMs to date rely on metal-dielectric composites and resonance phenomena. Dispersive behavior of NIMs implies large losses that could hinder their application to imaging. Such metamaterials typically consist of a periodic array of unit cells, encapsulating elementary structures, e.g., a split-ring resonator [5], a pair of nanorods [6], etc. The properties of

the metamaterial depend largely on the properties of the elementary structure within the unit cell. The structure of the unit cell is typically arranged from nanoengineered natural materials (elementary materials). An alternative approach of combining periodic unit cells with random metal-dielectric composites has been also reported [7]. The losses could be decreased by using low-loss elementary materials or through better designs of the elementary structure. In terms of loss, silver is the only available elementary plasmonic material. Although the losses can also be compensated through the use of an active gain medium [8], the loss compensation is indeed a challenging problem, which may not even be practical for certain applications. Hence, we have to rely on design optimization for bringing down the losses to the lowest possible levels.

Although NIMs based on periodic metal-dielectric composites are of colossal importance for overcoming the diffraction limit in modern optical systems, approaches to the controlled optimal design and consequent actual manufacturing of NIMs are currently in development. Normally, the design of a periodic NIM begins with the basis unit cell, which consists of resonant and nonresonant components geared toward providing specific properties to the entire array. Typically, the basis cell is chosen *a priori* and in many cases is obtained through physical intuition and knowledge of the basis resonant elements, like a split-ring resonator, a pair of coupled silver strips, or a pair of nanorods. The material properties for the various regions of the structure are usually limited by the availability of elementary materials. The dimensions of the basis structure are usually the most flexible parameters in the design, which is limited only by the fabrication tolerances. The dimensions, along with the material properties, form a hyperspace for the global optimization problem. The optimization problem consists of finding the

best point in this hyperspace with respect to a particular figure of merit.

An optimization technique must take into account the constraints on the various dimensions in the structure based on its manufacturability. The deviations in the optical properties of the actual nanoengineered elementary material from those in the bulk material should also be taken into account. In resonant structures, these deviations are sensitive to both a given fabrication process and a chosen design geometry. For example, a metallic resonator may have a larger loss compared to the loss of the same metal in bulk owing to its absolute geometrical scale (size effect), and its quality (surface roughness, structural inhomogeneities, etc.). Experimental examples of a particular wavelength-dependent adjusting of the bulk material properties are discussed in [9]. In contrast with [9], where feedback from fabrication to design optimization is discussed, this paper focuses on nature-inspired techniques for optimizing an optical metamaterial for NFL and a design for low-loss NIM.

The technique for the ultimate NFL design is based on simulated annealing (SA), a known heuristic approach to global optimization. As a proof-of-concept test the paper shows a simplified example utilizing SA for the ultimate design of a three-layer metamaterial with the lowest refractive index and the lowest loss. For the design of optical NIMs the SA method is compared with two other robust stochastic techniques, the genetic algorithm (GA) and particle swarm optimization (PSO). A basis 2D NIM structure defined in [7] and shown in Fig. 1 is used as a starting point. Specific behavior of the NIM structure with respect to variations in the design parameters is not well understood, which makes the application of computerized optimization schemes very attractive. The actual simulation in the optimization process is performed using numerical solvers based on two different methods, namely periodic finite element-boundary integral (PFEBI) method and spatial harmonic analysis (SHA). In this paper the GA is linked with the PFEBI solver, whereas SA and PSO rely on the SHA solver, for the electromagnetic simulations.

Section 2 describes in short the numerical solvers (PFEBI and SHA) that are used in this work. Section 3

gives an overview of the methods used in the optimization process (GA, PSO, and SA). Section 4 depicts the optimum results obtained with the three different approaches. Section 5 gives a summary of current studies and outlines the future work.

2. NUMERICAL SOLVERS

A very important component in any stochastic optimization process is a solver that is used for evaluating the fitness of a particular design. The solver is usually the bottleneck in the entire process, and a fast solver is of utmost importance for any realistic optimization goal. In this paper two different numerical solvers (PFEBI and SHA) are used in conjunction with the optimization tools.

A. Periodic Finite Element-Boundary Integral Method

The PFEBI [10] method is a modified version of the finite element-boundary integral (FEBI) method [11], where periodic boundary conditions have been imposed. In this technique, equations for the unknown electric or magnetic field values inside the computational domain are obtained from the differential form of Maxwell's equations. On the computational boundary, the unknown fields are expanded in terms of known basis functions. The field values from these two computational domains are coupled through integral equations on the boundary, leading to a system of linear equations that can be solved numerically for the unknown field values. The PFEBI method employed in this work uses brick elements and edge-based basis functions [11]. Moreover, the PFEBI method has been recently combined with a robust GA technique with the goal of evolving optimal designs for all-dielectric frequency selective surfaces (FSS) [12].

B. Spatial Harmonic Analysis

SHA [13] is a fast semi-analytic method for simulation of periodic structures. It is based on the expansion of the electromagnetic fields in terms of plane waves as given by Bloch's theorem. The structure to be simulated is divided into layers such that the material properties within a layer are invariant along the direction perpendicular to the layer. The eigenmodes within each layer are expressed as a summation of different plane wave modes as given by Bloch's theorem. The material properties for each layer are expressed as a Fourier series. These substitutions convert the Maxwell's equation into an eigenvalue equation that can be solved to yield the eigenmodes and corresponding eigenvalues for each layer. This is followed by application of boundary conditions at the interfaces between the layers to yield the electromagnetic fields throughout the structure.

3. OPTIMIZATION METHODS

A. Simulated Annealing

One of the design techniques tested in this study is simulated annealing (SA), a known heuristic approach to global optimization. SA is formally built upon a physical analogy of cooling crystal structures that spontaneously attempt to arrive at a global minimum [14]. The core com-

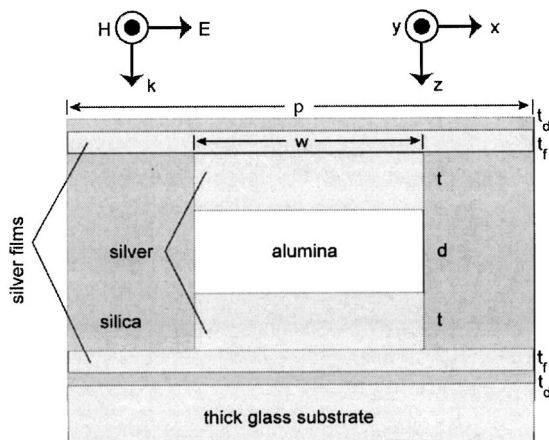


Fig. 1. Unit cell structure of the 2D periodic NIM grating geometry. The structure is illuminated by a monochromatic plane wave at normal incidence from air.

ponents of the SA method are an objective function F (error function, cost, etc.), a random generator of new solutions, and adjustable acceptance probability (usually Boltzmann probability) $p=e^{-\Delta F/T}$ for $\Delta F>0$, $p=1$ otherwise. A solution is a set of parameters to be optimized. The control variable T (temperature) is initially set to a high value, which results in almost free movements in the entire parameter space, and then decreased gradually, which leads to a more localized search. Although there is no direct physical analogy to the crystallization and equilibrium process in the ultimate design of NFL or NIMs (as in practically in any other of optimal design areas), the method is applicable to the continuous global optimization problem.

B. Genetic Algorithm

The GA [15,16] is another powerful optimization methodology that is based on the principles of natural selection and survival-of-the-fittest in genetic evolution. First, an initial population is formed where each of the individuals comprising the population corresponds to a specific realization of the design to be optimized in a given parameter space. A cost (to be minimized) or a fitness (to be maximized) is assigned to each individual to quantify its performance. Best-performing individuals in a generation are allowed to “mate” to produce the next generation of individuals. This process is repeated until convergence is achieved. During the computerized evolution process, a mutation operator is typically introduced to prevent the fitness from converging to local extrema rather than to the global extremum. The GA has been used extensively to synthesize novel metamaterials in the microwave regime such as artificial magnetic conducting (AMC) surfaces [17], metaferrites [18], and materials that exhibit zero or near-zero refractive index behavior [19]. More recently, the GA has been used to optimize the design of multiband metallodielectric FSS filters for IR applications [20].

C. Particle Swarm Optimization

Swarm intelligence is one of the latest nature-based stochastic optimization techniques that was recently introduced by Kennedy and Eberhart [21]. The researchers studied the social behavior of animals and insects in groups, such as swarms of bees, schools of fish, or flocks of birds. In essence, a swarm of bees, for example, is a decentralized social structure where the knowledge is matured by the individuals but perfected via information sharing. This relatively simple but flexible and robust optimization algorithm can be easily applied to the solution of many complex engineering problems.

Although the driving force behind the GA is competition, the driving force in PSO is cooperation [22,23]. In simplest terms, the individuals, i.e., particles, fly through the multidimensional search space and land at different coordinates. Each particle has its own position and velocity vectors. Moreover, a collection or swarm of particles is defined, where each particle is assigned a random position in the m -dimensional problem space so that each particle’s position corresponds to a candidate solution of the optimization problem. Based on the goodness of the position, each particle is assigned a fitness (or cost), and opti-

mization is further continued via the velocity operator. Each particle keeps a record of its personal best location as well as the best location for the entire swarm (i.e., the fittest particle in the swarm). The simplest form of the velocity operator is given by

$$V_{i,m}^{next} = (\omega V_{i,m}^{current}) + c_1^{rand}(p_{i,m}^{best} - X_{i,m}^{current}) + c_2^{rand}(g_m^{best} - X_{i,m}^{current}), \quad (1)$$

where $V_{i,m}^{next}$ is the updated velocity for the i th particle in dimension m , ω is the nostalgia constant, $V_{i,m}^{current}$ is the current velocity for the i th particle in dimension m , c_1^{rand} and c_2^{rand} are randomly generated constants, $X_{i,m}^{current}$ is the current position of the i th particle in dimension m , $p_{i,m}^{best}$ is the personal best coordinate of the i th particle in dimension m , and g_m^{best} is the global best of the entire swarm in the same dimension. The position update equation corresponding to Eq. (1) is given by

$$X_{i,m}^{next} = X_{i,m}^{current} + (\Delta t \times V_{i,m}^{next}), \quad (2)$$

where $X_{i,m}^{next}$ is the updated position in dimension m and the time step, Δt , is typically chosen to be unity for simplicity.

4. RESULTS

A. SA: Details and Results

As a proof-of-concept test consider a simplified example utilizing the selected heuristic method (SA) to the adaptive parametric design of an ultimate three-layer NFL with the lowest refractive index and the lowest loss. Specifically, the objective function is $F=n'|n|$. First, the initial arrangement of elementary materials was limited to two identical homogeneous layers of metal (silver) separated by a homogeneous dielectric spacer (silica). Next, two continuous parameters were introduced: (1) the thickness of each metal layer (Δ_m), ranging from 10 to 100 nm, and (2) the thickness of the spacer (Δ_s) 10–300 nm. Each value of F is obtained from a test run within the spectral range of 0.2–1.5 μm (the lowest F and a corresponding wavelength λ were selected within each wavelength sweep). Finally, after the selected random moves, the ultimate pair of parameters ($\Delta_m=19$ nm and $\Delta_s=85$ nm) was obtained for the optimal value of $n=0.04+0.23i$ at the wavelength of $\lambda \approx 478$ nm. Although the refractive index in the optimal NFL is positive, the result sets a reference for the values of effective n' (and the absorbance) achievable in a three-layer metal-dielectric structure.

A brute-force test is used to validate the results of the SA approach, as shown in Fig. 2. The figure combines a color contour plot indicating the values of the objective function ($F=n'|n|$) with the other contour plot of λ shown as the curves of uniform color. The values of F are indicated with a grayscale bar, while the values of the optimal wavelengths (λ) for a given value of F are indicated by the numbers next to the curves. The figure shows that the brute-force results are in excellent agreement with the SA approach; the simple two-dimensional parameter space has been intentionally taken to simplify the validation.

The SA algorithm is then applied to NIM optimization. Four of the geometrical parameters for the NIM were con-

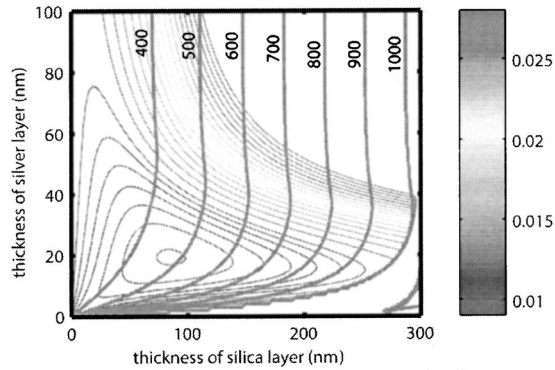


Fig. 2. Brute-force test of the SA approach to a NFL optimization. The grayscale contour plot indicates the values of the objective function. The values of wavelength (numbered lines of a second contour plot) are shown superimposed on top of the plot.

strained to vary between a minimum and a maximum value (i.e., $50 \text{ nm} \leq p \leq 500 \text{ nm}$, $20 \text{ nm} \leq w \leq p$, $20 \text{ nm} \leq t \leq 60 \text{ nm}$, and $20 \text{ nm} \leq d \leq 100 \text{ nm}$). The two remaining parameters T_d and T_f were both fixed at 20 nm. This choice of T_f was made to guarantee that the silver used in the NIM forms a continuous layer. The objective function is defined as

$$obj = 10 - \max_{\lambda}(-n'/n''), \quad (3)$$

since SA requires a positive objective function, and its evaluations were performed by the 2D SHA method. For the NIM design considered here, the maximum value of the fitness and the corresponding wavelength were found to lie within the range of $400 \text{ nm} \leq \lambda \leq 800 \text{ nm}$.

When recovering $n = n' + in''$ from the complex reflection and transmission coefficients, there is an ambiguity that arises in the determination of n' . This ambiguity is due to the multivalued nature of the arc-cosine function that appears in the inversion algorithm [24,25]. To remove this ambiguity, continuity of n' is enforced with respect to wavelength from the long wavelength limit, where the NIM structure should exhibit nonmagnetic behavior (i.e., $\mu \rightarrow 1$). For this purpose, the wavelength is scanned from 1600 nm down to 800 nm, reducing the sampling wavelength by 10% at each step. Next, the numerical difference of n' is taken between neighboring frequency points within this range. If the difference is above a preset threshold, an intermediate frequency point is chosen for additional sampling. This process is repeated until a smooth curve is obtained for n' , which leads to an unambiguous value at 800 nm. Within the optimization range, the frequency is sampled at a fixed 10 nm interval.

The optimum design obtained by SA is $p = 323.6 \text{ nm}$, $w = 181.6 \text{ nm}$, $t = 40.2 \text{ nm}$, and $d = 80.1 \text{ nm}$ with the effective index $n = -0.83 + i0.22$ at $\lambda = 770 \text{ nm}$, corresponding to a figure of merit 3.79. The reflectance, transmittance, and absorbance are very close to spectra plotted for GA in Fig. 3, and the effective refractive index is plotted in Fig. 4.

B. GA: Details and Results

Next, the specific details of the GA optimization procedure developed for the NIM designs reported here are discussed. The geometrical constraints for GA optimization of the NIM design are the same as those used in SA. A

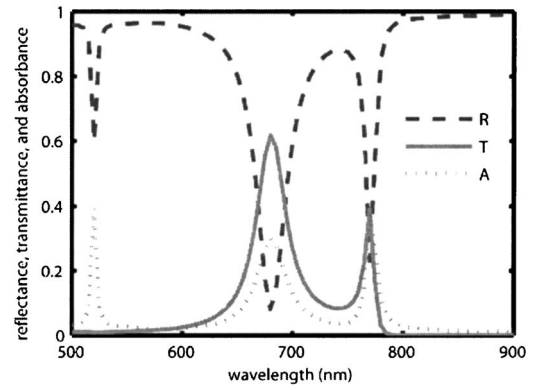


Fig. 3. Reflectance (R), transmittance (T), and absorbance (A) spectra of the GA-optimized NIM structure.

specific implementation of the GA, called the micro GA [26], with a population size of six was used in this study. The fitness/cost function used in the GA is defined by

$$fitness = -cost = \max_{\lambda} \{-n'/n''\}. \quad (4)$$

In other words, the design objective is to achieve a large negative index of refraction together with the lowest possible loss. Fitness evaluations for GA were performed using the PFEBI method. The PFEBI analysis used for each individual population member had a basic brick element size of $20 \text{ nm} \times 20 \text{ nm} \times 20 \text{ nm}$, guaranteeing that an element edge would not exceed $\lambda/10$ at any wavelength within the simulation range. With the NIM design parameter ranges and the brick element size given above, the total number of unknowns in the matrix equation for the PFEBI system ranges from 69 (21 elements) to 1175 (375 elements).

Figures 3–6 show the spectra and the effective parameters of the GA-optimized NIM structure. The optimum geometrical parameters in this case were found to be $p = 314.3 \text{ nm}$, $w = 176.8 \text{ nm}$, $t = 42.9 \text{ nm}$, and $d = 72.1 \text{ nm}$. Convergence to the maximum fitness of 3.25 was achieved at generation 87. The corresponding wavelength is 770 nm, and the equivalent index of refraction is equal to $n = -0.810 + i0.249$. Two distinct peaks in T can be observed in Fig. 3. Only the second peak at 770 nm, is associated with negative index of refraction, reaching a level of 39%. The optimized structure features a negative index

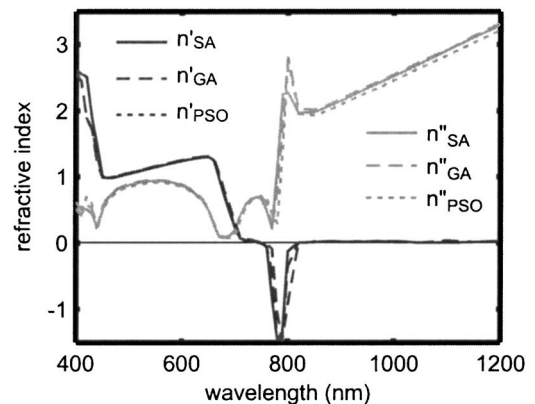


Fig. 4. Real and imaginary parts of the effective index of refraction n of the optimized structure.

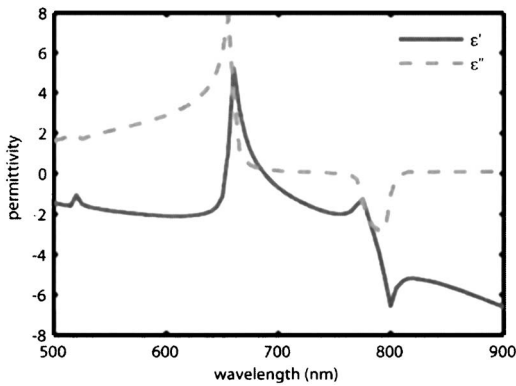


Fig. 5. Real and imaginary parts of the recovered effective permittivity of the optimized structure.

of refraction from 750 to 810 nm, as shown in Fig. 3. This range for $n' < 0$ extends over the region where both $\epsilon' < 0$ and $\mu' < 0$ are achieved simultaneously (see Figs. 4 and 5). However, n'' sharply decreases when both conditions are met, and $\mu' < 0$ is accompanied by sharp increase in A . It is this minimization of n'' over the narrow bandwidth that leads to the maximization of the fitness at 770 nm.

C. PSO: Details and Results

Another optimization was performed by the PSO method to minimize the cost defined in Eq. (3) using the same parameter ranges that were defined for the GA. In order to make a fair comparison with the GA, the PSO was started with a swarm of six particles and was run for 100 iterations. The velocity was limited to be in the range of $-0.3 \leq vel \leq 0.3$ to prevent the particles from taking impractical steps over the search space. Fitness evaluations for the PSO were performed by the 2D SHA method. PSO converges to the minimum cost of -3.23 achieved at a wavelength of 780 nm with only 35 iterations. The optimized parameters were found to be $p=328.7$ nm, $w=168.0$ nm, $t=45.8$ nm, and $d=68.0$ nm. These values are close to those found by the GA, although they are not exactly the same. However, it is noted that the optimized fitness values for the two methods are very close to each other. The spectra of the effective parameters for the PSO-optimized NIM structure are essentially the same as those of the GA-optimized structure shown in Figs. 3–6.

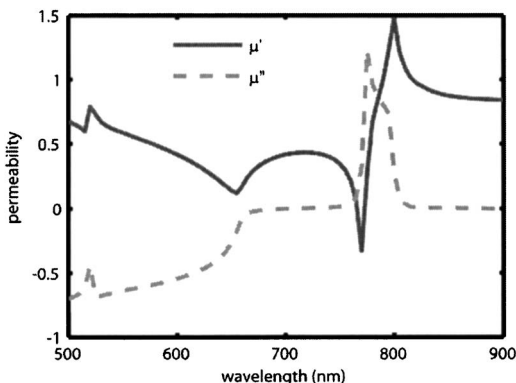


Fig. 6. Real and imaginary parts of the recovered effective permeability of the optimized structure.

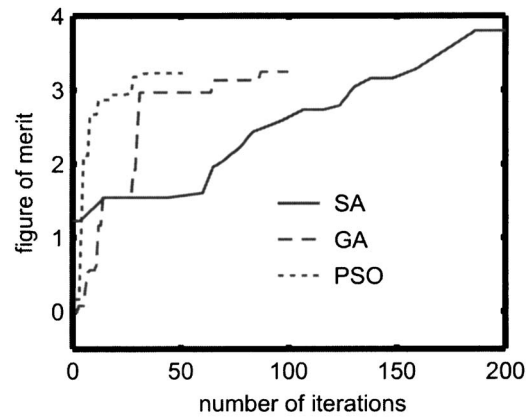


Fig. 7. Comparison of convergence properties of the SA, GA, and PSO optimization methods.

The optimized NIM designs obtained by the three stochastic methods are similar. Convergence curves for the GA, PSO, and SA methods for this particular optimization problem are compared in Fig. 7. The population size for GA and the number of particles for the PSO are both six, so each increment in the horizontal axis corresponds to six additional evaluations of the fitness function. Because the number of evaluations of the objective function at each temperature for SA is not fixed, we used the total numbers of evaluations of SA divided by six as the horizontal axis to make a fair comparison. It is observed that in this particular case the PSO converges much faster than the other two methods.

5. SUMMARY

We have demonstrated the successful optimization of an optical NIM design through three different stochastic optimization tools; GAs, PSO, and SA. SA gives a maximum figure of merit 3.79. A maximum fitness (figure of merit) parameter ($-n'/n''$) of 3.25 was obtained through GA after 87 generations, where each generation had six individuals. With PSO, a fitness parameter of 3.23 was obtained after only 35 iterations with six particles.

We also note that in order to achieve optimum designs that could be realized with the available fabrication technology, the fabrication constraints should be incorporated into the optimization process. The fabrication constraints could include geometrical constraints, i.e., the lowest dimension and accuracy that could be achieved. It could also include constraints on material properties, since only a limited number of materials are good candidates in the fabrication process. The fabrication process could itself alter the properties of the elementary materials, resulting in more loss compared to bulk material. This variation in material properties has to be taken into account through feedback from fabrication and measurements [27].

In spite of using fast solvers each fitness evaluation takes a substantial amount of time. This will be worse for three-dimensional systems because of the increased complexity. This problem could be alleviated by incorporating the principles of system identification into the optimization routine. System identification is routinely used in control systems to model the behavior of a complicated system in terms of a simpler model. System identification

could help the optimization routine reach the optimum with fewer iterations, but as an added and more vital advantage, it would also provide us with an understanding of the dependence or sensitivity of desired properties on various parameters.

ACKNOWLEDGEMENTS

We would like to cite fruitful discussions with V. P. Drachev. This work was supported in part by Army Research Office (ARO) grant W911NF-04-1-0350, National Science Foundation (NSF)–Nanoscale Interdisciplinary Research Team award ECS-0210445, ARO–Multidisciplinary University Research Initiative award 50342-PH-MUR, the Penn State Materials Research Institute, and by the Penn State Materials Research Science and Engineering Center under NSF grant DMR 0213623.

REFERENCES

- J. B. Pendry, "Negative refraction makes a perfect lens," *Phys. Rev. Lett.* **85**, 3966–3969 (2002).
- W. Cai, D. A. Genov, and V. M. Shalaev, "Superlens based on metal-dielectric composites," *Phys. Rev. B* **72**, 193101 (2005).
- N. Fang and X. Zhang, "Imaging properties of a metamaterial superlens," *Appl. Phys. Lett.* **82**, 161–163 (2003).
- D. Melville and R. Blaikie, "Super-resolution imaging through a planar silver layer," *Opt. Express* **13**, 2127–2134 (2005).
- J. B. Pendry, A. J. Holden, D. J. Robbins, and W. J. Steward, "Magnetism from conductors and enhanced nonlinear phenomena," *IEEE Trans. Microwave Theory Tech.* **47**, 2075–2084 (1999).
- V. M. Shalaev, W. Cai, U. K. Chettiar, H.-K. Yuan, A. K. Sarychev, V. P. Drachev, and A. V. Kildishev, "Negative index of refraction in optical metamaterials," *Opt. Lett.* **30**, 3356–3358 (2005).
- U. K. Chettiar, A. V. Kildishev, T. A. Klar, and V. M. Shalaev, "Negative index metamaterial combining magnetic resonators with metal films," *Opt. Express* **14**, 7872–7877 (2006).
- T. A. Klar, A. V. Kildishev, V. P. Drachev, and V. M. Shalaev, "Negative-index metamaterials: going optical," *IEEE J. Sel. Top. Quantum Electron.* **12**, 1106–1115 (2006).
- A. V. Kildishev, U. K. Chettiar, H.-K. Yuan, W. Cai, and V. M. Shalaev, "Optimizing optical negative index materials: feedback from fabrication," in *Proceedings of the 23rd International Review of Progress in Applied Computational Electromagnetics* (Applied Computational Electromagnetics Society, 2007), pp. 11–16.
- T. F. Eibert, J. L. Volakis, D. R. Wilton, and D. R. Jackson, "Hybrid FE/BI modeling of 3-D doubly periodic structures utilizing triangular prismatic elements and an MPIE formulation accelerated by the Ewald transformation," *IEEE Trans. Antennas Propag.* **47**, 843–850 (1999).
- J. L. Volakis, A. Chatterjee, and L. C. Kempel, *Finite Element Method for Electromagnetics* (IEEE, 1998).
- L. Li and D. H. Werner, "Design of all-dielectric frequency selective surfaces using genetic algorithms combined with the finite element-boundary integral method," in *Proceedings of the Antennas and Propagation Society International Symposium and USNC/URSI National Radio Science Meeting*, Vol. 4A, (IEEE, 2005), pp. 376–379.
- A. V. Kildishev and U. K. Chettiar, "Cascading optical negative index metamaterials," *J. Appl. Comput. Electromagnetics Soc.* **22**, 172–183 (2007).
- D. T. Pham and D. Karaboga, *Intelligent Optimization Techniques* (Springer-Verlag, 2000).
- R. L. Haupt and S. E. Haupt, *Practical Genetic Algorithms* (Wiley-Interscience, 2004).
- Y. Rahmat-Samii and E. Michelssen, eds., *Electromagnetic Optimization by Genetic Algorithms* (Wiley-Interscience, 1999).
- D. J. Kern, D. H. Werner, A. Monorchio, L. Lanuzza, and M. Wilhelm, "The design synthesis of multiband artificial magnetic conductors using high impedance frequency selective surfaces," *IEEE Trans. Antennas Propag.* **53**, 8–17 (2005).
- D. J. Kern, D. H. Werner, and M. Lisovich, "Metaferrites: using electromagnetic bandgap structures to synthesize metamaterial ferrites," *IEEE Trans. Antennas Propag.* **53**, 1382–1389 (2005).
- M. A. Gingrich and D. H. Werner, "Synthesis of low/zero index of refraction metamaterials from frequency selective surfaces using genetic algorithms," *Electron. Lett.* **41**, 1266–1267 (2005).
- J. A. Bossard, D. H. Werner, T. S. Mayer, J. A. Smith, Y. U. Tang, R. Drupp, and L. Li, "The design and fabrication of planar multiband metalodielectric frequency selective surfaces for infrared applications," *IEEE Trans. Antennas Propag.* **54**, 1265–1276 (2006).
- J. Kennedy and R. C. Eberhart, *Swarm Intelligence* (Academic, 2001).
- D. W. Boeringer and D. H. Werner, "Particle swarm optimization versus genetic algorithms for phased array synthesis," *IEEE Trans. Antennas Propag.* **52**, 771–779 (2004).
- D. W. Boeringer and D. H. Werner, "Efficiency-constrained particle swarm optimization of a modified Bernstein polynomial for conformal array excitation amplitude synthesis," *IEEE Trans. Antennas Propag.* **53**, 2662–2673 (2005).
- D. R. Smith, S. Schultz, P. Markoš, and C. M. Soukoulis, "Determination of effective permittivity and permeability of metamaterials from reflection and transmission coefficient," *Phys. Rev. B* **65**, 195104 (2002).
- A. V. Kildishev, W. Cai, U. K. Chettiar, H.-K. Yuan, A. K. Sarychev, V. P. Drachev, and V. M. Shalaev, "Negative refractive index in optics of metal-dielectric composites," *J. Opt. Soc. Am. B* **23**, 423–433 (2006).
- S. Chakravarty, R. Mittra, and N. R. Williams, "Application of a micro-genetic algorithm (MGA) to the design of broadband microwave absorbers using multiple frequency selective surface screens buried in dielectrics," *IEEE Trans. Antennas Propag.* **50**, 284–296 (2002).
- H.-K. Yuan, U. K. Chettiar, W. Cai, A. V. Kildishev, A. Boltasseva, V. P. Drachev, and V. M. Shalaev, "A negative permeability material at red light," *Opt. Express* **15**, 1076–1083 (2007).